Chloride diffusion and oxygen permeability of mortars with low active blast furnace slag

Ahmed Hadj-sadok [a], Luc Courard [b,]

[a] GEE laboratory, High National School of Hydraulic (ENSH), Blida, Algeria

[b] GeMMe Sector, ArGEnCo Department, Urban and Environmental Engineering, University of Liège, Belgium

---

ABSTRACT

Depending on its hydraulic activity, the use of Granulated Blast Furnace Slag (GBFS) in cementitious materials contributes to improve their durability performances. In this paper, a low reactive Granulated Blast Furnace Slag with is used in modifying mortar composition. Some durability properties of mixes containing 0, 30 and 50% of slag as substitution to OPC are studied. Diffusion and conduction of chlorides at long term are analyzed with different initial wet curing periods. Microstructure of mortars after 360 days of diffusion is observed by means of Mercury Intrusion Porosimetry. The oxygen permeability is analysed at 90 and 360 days of wet curing. The results indicate good performances to chloride diffusion of the mortars with GBFS, especially for a prolonged wet curing. Moreover, the GBFS are inefficient for oxygen permeability at 90 days but they however allow a decreasing over long term.

Keywords: Environment, mortar, granulated blast furnace slag, mercury intrusion porosity, oxygen permeability, chloride diffusion, conduction.

Highlights:

- Mortars with GBFS show the greatest resistance to chloride ion diffusion and a good linear correlation is found between the diffusion coefficient and total charge.
- The initial period of wet curing influences the resistance to chloride diffusion of mortars with GBFS.

- At long term, oxygen permeability of mortars with GBFS is improved compared to the OPC mortars.
- After 360 days of maturation, a densification of mortars with GBFS microstructure is observed even after diffusion test.

* Corresponding author. Tel.: +213 561 35 42 44; Fax: +213 25 29 90 37
E-mail address: a.hadjsadok@ensh.dz (A. Hadj sadok)

Introduction

The use of granulated blast furnace slag (GBFS) as a cement additive contributes to increase cement production and improve its technical performances while preserving the environment. However, the steel industry produces a very variable quality of slags in terms of chemical composition and glass contents, which directly affects the hydraulic activity of slag [1,2]. When mixed with the clinker, the slag reacts with the calcium hydroxide and forms additional hydrated and this leads to an improvement in the chemical resistance and microstructure [3,4].

Moreover, in literature, several studies report a considerable improvement in transport properties (capillary absorption, permeability and diffusion) of mortars and concretes based on GBFS binder [6-8]. However, this highly depends on the hydration of the slag and consequently on its hydraulic activity.

The durability properties and microstructure of matrices based on cements slag are significantly influenced by the curing conditions (relative humidity and temperature), especially if the slag is slightly reactive. Ortega J.M. et al [9] observed a significant decrease of capillary absorption and chlorides diffusion of CEM III type mortars with prolonged high relative humidity curing. This was attributed to the minimizing drying

action and the improvement of water availability for clinker-slag hydration reactions. In another study [10], the same researchers studied the effect of different curing environments (Atlantic and Mediterranean climates) on the chlorides migration in CEM III and OPC mortars. The results showed a good performance regarding chloride ingress resistance in CEM III even in the non-optimal cure environments studied, after an enough maturing time.

Several studies have shown higher performances of cement slag mixtures against chloride attack with regard to OPC based mixtures [11-14]. By testing concrete blocks exposed in a natural marine site, Abd El Fattah [15] et al showed a good influence of the slag on chloride penetration and corrosion mitigation. This is often attributed to the improved chlorides binding capacity of hydrates [16]. Florea and Brouwers [17] found that CSH and CAH hydration phases are responsible for about two-thirds of fixing of chloride ions in matrix of cement slag mixtures. However, this binding capacity remains sensitive to the slag composition and to maturity degree.

Natural diffusion test inducing only gradients concentration, even if it is a laborious test, is generally considered to represent the penetration mechanism of chloride ions in concrete with most precision under real conditions of exposure [18]. The ASTM C1202 Conduction Test [19] is commonly used as accelerated test: although it does not yield a diffusion coefficient, it has the advantage of being fast and giving a good indication of chlorides diffusion. However, to see its effectiveness, it is always interesting to quantify the correlation between conduction and natural diffusion of chlorides, in particular in the case of unconventional binder.

In a previous study **[20]**, we examined the microstructure and some durability aspects of mortars containing up to 50% of GBFS with low reactivity index. The results indicated finer porosity and lower water absorption for mortars with GBFS at old ages (90 and 360

days). Moreover, after 90 days of wet curing and 270 days of chloride diffusion, lower diffusion coefficient has been observed for 50% slag substitution level. The present work is a continuity of this previous research and thus, the effect of the wet curing before the diffusion test (90 and 180 days) is presently studied, in comparison to the previous work when only 90-day period was considered. Moreover, the chlorides conduction and the study of the pores distribution of the matrices after diffusion are also studied. And finally, oxygen permeability has been recorded as additional durability index.

2. Experimental program

2.1 Materials

In this study, Ordinary Portland Cement (OPC) type CEM I 52.5 N with a fineness of 4200 cm^2/g was used for mortar mixes. Algerian Granulated Blast Furnace Slag (GBFS) was used in this work. It was ground in a laboratory mill to a Blaine fineness of 4150 cm^2/g. A broad characterization of this slag was carried out in previous studies [3, 20] which showed its low rate of alumina and magnesia contents as well as its low hydraulic reactivity. The chemical composition of cement and slag are given in Table 1. Standardized sand with maximum particle size of 2 mm was used for mortars mixes.

2.2 Mixtures properties and curing procedures

The mortar mixes (M0, M30 and M50) have a Sand to Binder ratio of 3:1 and Water/Binder (W/B) ratio of 0.5. The binder for mortar M0, M30 and M50, was obtained by partial substitution of cement with 0, 30 and 50% of slag, respectively. Substitution was made by mass of cement. Mortars specimens were cast according to European Standard EN 196-1 [21]. They were demoulded after 24 h and cured in moist room at 20 ± 2°C and more than 95% relative humidity until the age of testing. Properties (compressive strength and water water absorption by immersion P_W) of hardened mortars with and without GBFS are shown in table 2 [20].

112 ***2.3 Test procedures***

113 *2.3.1 Chloride permeability tests*

114 *2.3.1.1 Steady state diffusion test*

115 Rates of diffusion of Cl^- ions into mortars are monitored using two compartment diffusion
116 cells. 8 mm thick mortar blocks are sawed from 80 mm diameter specimens and stored in
117 $Ca(OH)_2$ saturated solution. Prior to the test, each specimen is polished with 600-grade
118 emery paper, rinsed with deionised water and surface dried with a tissue before being fitted
119 into the diffusion cell (Fig. 1). After fitting with epoxy resin and sealing with silicon paste,
120 the cells are filled at one side with $Ca(OH)_2$ solution and at the other side with 1 Mole
121 NaCl in a saturated $Ca(OH)_2$ solution [20]. At periodic intervals, chloride concentration is
122 determined by potentiometric titration from a 10 ml sample of the solution in cell 2. The
123 occurrence time (breakthrough time) was calculated from the intercept of the concentration
124 versus time date (minimum rate of 30 mg/l of Cl^- ions is reached in the cell 2). The
125 effective diffusion coefficient is calculated, when the steady state is reached, according
126 equation 1 (in m^2/s).

127

128 $$D_e = \frac{V_1}{A}\frac{\Delta C_1}{\Delta t}\frac{e}{(C_2 - C_1)} \quad (1)$$

129

130 With $\Delta C/\Delta t$: an increase of chloride concentration in cell 1, C_1 and C_2: chloride
131 concentrations of cells 1 and 2, A: section of mortar slices, e: thickness of mortar slices and
132 V_1: volume of cell 1.

133 The diffusion test was carried out on two sets of mortars preserved before the test during
134 90 and 180 days of wet curing. At 360 days of diffusion, samples of mortar were taken and
135 Mercury Intrusion Porosimetry tests were carried out.

136 *2.3.1.2 Conduction test*

The specimens of 96 mm diameter and 50 mm thick are conditioned by achieving vacuum pressure on the dry specimen and maintaining for 3 h, vacuum saturation for a period of 1 h after adding de-aerated water, and further soaking under water for a period of 18 h. The specimens were kept in a moist curing (95% RH, 20°C) environment during 90 and 180 days before performing the chloride conduction test (the rapid chloride permeability test), according to ASTM C 1202-94 standard [19].

2.3.2 Mercury Intrusion Porosimetry

In order to analyze pore size distribution, the different mortars have been examined by Mercury Intrusion Porosimetry (MIP). This test was carried out on two series of samples:

- Samples kept for 360 days of wet curing,
- Samples taken after 360 days of chloride diffusion.

For each mortar, three samples were tested. The measuring instrument used is a Pascal 240 porosimeter. The increasing step of pressure was fixed to 200 MPa, allowing investigation of pore radius from 7.5 μm to 3.7 nm. The test was performed on approximately 2 cm^3 mortar samples after drying at 50°C and in presence of silica gel until constant mass.

2.3.3 Oxygen permeability test

Oxygen permeability is determined on cored cylindrical mortar specimens (diameter 80 mm and height 40 mm) and ground on both sides. After maturation period (90 and 360 days), samples are dried in a ventilated oven for a minimum of 7 days at 45 °C until constant mass (less than 0.1% mass change in 24 h). The method used in this test is that known as "CEMBUREAU" [22].The test consists in subjecting the specimen to a constant pressure gradient and measuring the gas flow time in steady state through sample. Equation 2 allows calculating the permeability coefficient K for a given pressure Po. In this test, the absolute pressures applied to the samples are 1.6, 1.9 and 2.2 bars, respectively.

$$k = \frac{8.P_{a.}Q.H.\mu}{\pi.\Phi^2.(P_0^2.-.P_a^2)} \quad (m^2) \qquad (2)$$

Where *Pa*: atmospheric pressure, *Q*: volumetric flow rate, μ: dynamic viscosity of oxygen, H: thickness and Φ: diameter

3. Results and discussions

3.1 Chloride permeability

3.1.1 Steady state diffusion

The evolution of chloride diffusion has been measured during 360 days for mortars with and without GBFS, after 90 and 180 days of wet curing. Fig. 2 shows the evolution of the concentration of chloride ions in cell 2 versus time for the three mortars studied. The results showed a high diffusion rate for the OPC mortar in comparison to mortars with GBFS, for a tow initial cure period: for mortar with initial wet curing period of 90 days and after 360 days of diffusion, the concentration chloride reaches about 1400 mg/l for M0 compared to 520 mg/l and 70 mg/l for M30 and M50, respectively.

The effective diffusion coefficients and breakthrough times are presented in table 3. For 90 days initial curing, the diffusion of chloride ions through OPC mortar specimens is observed after only 45 days with an effective diffusion coefficient of 2.96×10^{-10} m²/s. The mortars with GBFS showed smaller chloride permeability. In fact, the breakthrough time is 73 and 220 days for M30 and M50, respectively and in comparison to OPC mortar, it represents a reduction of 60% and 93%, respectively.

The results of the pore size distribution for the three types of mortars at 360 days of maturation in wet curing are shown in Fig. 3 and the same results for 90 days wet curing followed by 360 days of chloride diffusion test are shown in Fig.4. Medium radius pore (r_m) and threshold pore access radius (r_t) of mortars are presented in Table 4.

185 The results presented in fig. 3 show similar pore geometrical characteristics (r_m and r_t) for
186 M0 and M30 mortars, even if the M30 develops a more refined pore network (especially
187 for the fraction with a diameter less than 50 nm). The porous structure of the M50 mortar is
188 narrower. A decrease of 11% in average radius and 12.5% of threshold radius compared to
189 the control mortar was recorded. This variation in microstructure may explain the
190 performance to chlorides diffusion of mortars with GBFS. In our case, it should be noted
191 that the presence of chloride ions in cement matrix of mortars did not too much influenced
192 the development of the microstructure of the mortars with GBFS. In fact, the densification
193 of mortars with GBFS microstructure, in particular M50, was as well observed in the
194 mortars subjected to chloride diffusion as for those which were conserved in wet curing
195 (Fig. 3, 4 and Table 4). The distribution of pores between 7 and 50 nm is more important
196 for M30 and M50 mortars. This range is mainly attributed to the fine capillary porosity and
197 the inter-crystallite porosity [5,23]. During hydration of GBFS, the pozzolanic reaction
198 consumes the $Ca(OH)_2$ of the cementitious matrix and leads in the formation of secondary
199 CSH gel indicated to be very effective in filling the capillary pores in matrix [24].

200 The improvement in diffusion is also attributed to the binding capacity by adsorption of
201 diffusing chlorides of the hydrates of slag (*CSH* and *CAH*) present in the pore walls and
202 offering a high specific surface [25-27]: Luoa et al [14] already observed an increase in
203 physical chlorides binding when cement was partially substituted by slag.

204 In our study, it should be noted that mortars have fairly large wet curing period of 90 or
205 180 days before being placed in diffusion cells. This cure conditions and the long test
206 period favours continuous hydration of slag allowing the densification of the matrix and
207 possibly the chloride binding capacity of slag hydrates.

208

209 *3.1.1.1 Influence of moist cure*

210 The increase in curing time before test (from 90 to 180 days) led to an improvement
211 in the resistance to chloride penetration of mortars with GBFS (M30 and M50) but not of
212 the reference mortar M0. This improvement is shown through an extension of time of
213 passage of Cl^- ions as well as a reduction of the diffusion coefficient.

214 Indeed, for M0 mortar, the difference in chlorides concentration remains small variable
215 (less than 10%) between the two initial cure cycles (90 and 180 days) at any age of the test,
216 up to 360 days (Fig.2). This variation is translated by 7 days increase in breakthrough time
217 and 6% decrease in diffusion coefficient (Table 3). On the other side, for M30 mortar,
218 there was a significant reduction in the chlorides concentration in the cell 2, in order of 50,
219 47 and 43% after 90, 180 and 360 days diffusion. The breakthrough time has thus
220 increased from 73 to 91 days, which corresponds to an increase of 25%. At the same time,
221 a reduction of about 43% of the diffusion coefficient was recorded. After 180 days of wet
222 curing and 360 days of diffusion, no chloride appearance was detected in cell 2 for M50,
223 which did not allowed measuring the breakthrough time and the diffusion coefficient. This
224 shows a particularly high resistance to chloride penetration for M50 mortar.

225 *3.1.1 Chloride conduction*

226 The results of chloride ions conduction test (ASTM accelerated test) are presented
227 for mortars with and without slag at 90 and 180 days in fig. 5.

228 A proportional decrease in the total charge Q with the rate of substitution is recorded at 90
229 as at 180 days. Several research studies [24, 28-30] have shown a low conduction of
230 chloride ions of concretes with GBFS, especially for high substitution rates (greater than
231 50%). The increase in curing period led to a decrease in the charge Q of 27 and 28% for
232 M30 and M50 mortars with GBFS, respectively. For M0, the decrease is negligible (2%).
233 Comparing these results with those of steady-state diffusion, we observe a similar

234 variation, even if the results with M50 mortar at 180 days curing could not be compared
235 because of its low diffusion. However, its low *Q* value (665 Coulomb) reflects its low
236 diffusion observed under steady-state test (fig. 2).

237 The fig. 6 present the relationship between the results of diffusion test (diffusion
238 coefficients) and conduction test (total charge *Q*) of mortars with and without slag at 90
239 and 180 days of wet curing. A very good linear correlation ($R^2 = 0.99$) shows a decrease of
240 the total charge with the decrease of diffusion coefficient.

241 ***3.2 Oxygen permeability***

242 The oxygen permeability results of M0, M30 and M50 mortars at medium (90 days) and
243 long terms (360 days) are shown in fig. 7. At 90 days, the lowest permeability is recorded
244 for M0 mortar. At this time, the permeability of mortar with 30% GBFS is slightly higher
245 than that of the control mortar (but the values remain comparable). The M50 recorded a
246 permeability increase of 32% compared to the mortar without addition. In long term (360
247 days), a different variation is observed. Indeed, the trend has reversed and a decrease in the
248 permeability with the increase of slag rate is observed. The mortars M30 and M50 showed
249 respectively a decrease of 21 and 31% compared with the control mortar.

250 This variation can be directly related to the refinement of porosity and the densification of
251 matrix due to the formation of additional CSH resulting from the slag hydration following
252 its activation by calcium hydroxide ($CaOH_2$), in particular at long term [20]. The
253 maturation period of 90 days was not sufficient for a good hydration of this poor reactive
254 GBFS and did not allow the microstructure to be sufficiently developed for the
255 improvement of the permeability of mortars. However, for slags with good hydraulic
256 reactivity, a better permeability performance of concretes is reported at 28 and 90 days
257 [6,31]. In our case, the beneficial effect was observed only at 360 days. This proves both

258 the low reactivity of the slag studied and the importance of the wet curing for improving
259 the durability of slag concretes.

260 **4. Conclusion**

261 The main conclusions to be drawn from the present experimental investigations are as
262 following:

263 • Chloride diffusion was studied by means of natural diffusion test during 360 days
264 after two initial curing periods (90 and 180 days). After 90 days initial wet curing,
265 in comparison with the control mortar, 30% of GBFS reduces the breakthrough
266 time, but no apparent difference was observed in the diffusion coefficient.
267 However, 50% slag leads to a very significant reduction in the breakthrough time
268 and diffusion coefficient. The increase of the initial cure period leads to a
269 systematic reduction of the diffusion in mortars with GBFS. The performances of
270 the reference mortar was not influenced by the curing period;

271 • The observation of the microstructure after 360 days shows that mortars with GBFS
272 develop refined pore network which is consisting essentially with fraction pores of
273 radius less than 50 nm reflecting a densification of microstructure. Moreover, the
274 presence of chloride ions in matrix did not too much influence the development of
275 microstructure of the mortars with GBFS;

276 • Low chloride conduction is observed for mortars with GBFS compared with the
277 OPC based mortar. Conduction test results show a similar trend to those of the
278 steady-state diffusion test. A very good linear correlation is obtained between total
279 charge Q and diffusion coefficient;

- At 90 days, while a substitution rate of 50% slag leads to an increase in oxygen permeability, the 30% slag rate affects it only slightly. On the contrary, at long term (360 days) mortars with GBFS are less permeable to oxygen.

References

[1]. Pal S, Mukherjee A, Pathak S. Investigation of hydraulic activity of ground granulated blast furnace slag in concrete. Cem Concrete Res 2003;33(9):1481-1486.

[2]. Bougara A, Lynsdale C, Milestone NB. Reactivity and performance of blast furnace slags of differing origin. Cem Concrete Comp 2010;32(4): 319-324.

[3]. Hadj Sadok A, Kenai S, Courard L, Michel M, Khatib D. Durability of mortar and concretes containing slag with low hydraulic activity. Cem Concrete Comp 2012;34(5):671-677.

[4]. Thomas MDA, Scott A, Bremmer T, Bilodeau A, Day D. Performance of slag concrete in marine environment. ACI Mater Journal 2008;105(6):628-634.

[5]. Ye G, Van Breugel K. Simulation of connectivity of capillary porosity in hardening cement-based systems made of blended materials. Concr Tech 2009;54(2):163-184.

[6]. Guneyisi E, Gesoglu M. A study on durability properties of high-performance concretes incorporating high replacement levels of slag. Mater Struct 2008;40(3):479-493.

[7]. Shi HS, Xu BW, Zhou XC. Influence of mineral admixtures on compressive strength, gas permeability and carbonation of high performance concrete. Constr Build Mater 2009;23(5):1980–1985.

301 [8]. Chen H-J, Huang S-S, Tang C-W, Malek M.A, Ean L-W. Effect of curing
302 environments on strength, porosity and chloride ingress resistance of blast furnace slag
303 cement concretes: A construction site study. Constr Build Mater 2012; 35:1063-1070.

304

305 [9]. Ortega JM, Sánchez I, Climent MA. Durability related transport properties of OPC
306 and slag cement mortars hardened under different environmental conditions. Constr Build
307 Mater 2012;27(1):176-183.

308 [10]. Ortega JM, Sánchez I, Climent MA. Influence of different curing conditions on the
309 pore structure and the early age properties of mortars with fly ash and blast-furnace
310 slag. Mater Constr 2013; 63(310):219-234.

311 [11]. Geiseler J, Kollo H, and Lang E. Influence of blast furnace cements on durability of
312 concrete structures. ACI Mater J 1995, 92(3):252–257.

313 [12]. Yuan Q, Shi C, De Schutter G, Audenaert K, Deng D. Chloride binding of cement
314 based materials subjected to external chloride environment – a review. Constr Build Mater
315 2009;23(1):1-13.

316 [13]. Arya C, Xu Y. Effect of cement type on chloride binding and corrosion of steel in
317 concrete. Cem Concr Res 1995;25:893–902.

318 [14]. Luoa R, Caib Y, Wangb C, Huanga X. Study of chloride binding and diffusion in
319 GGBS concrete. Cem Concrete Res 2003;33(1):1-7.

320 [15]. Abd El Fattah A, Al-Duais I, Riding K, Thomas M. Field evaluation of corrosion
321 mitigation on reinforced concrete in marine exposure conditions. Constr Build Mater
322 2018;165, 663-674.

323 [16]. Dhir RK, EL-Mohr MAK, Dyer TD. Chloride binding in GGBS concrete. Cem
324 Concrete Res1996;26(12):1767-1773.

325 [17]. Florea MVA, Brouwers HJH. Modelling of chloride binding related to hydration
326 products in slag-blended cements. Constr Build Mater 2014;64:421-430

327 [18]. Van Noort R, Hunger M, Spiesz P. Long-term chloride migration coefficient in slag
328 cement-based concrete and resistivity as an alternative test method. Constr Build Mater
329 2016;115:746-759.

330 [19]. ASTM C1202-10, Standard test method for electrical indication of concrete's ability
331 to resist chloride ion penetration, ASTM Int. USA: 2010.

332 [20]. Hadj Sadok A, Kenai S, Courard L, Darimont A. Microstructure and durability of
333 mortars modified with medium active blast furnace slag. Constr Build Mater
334 2011;25(2):1018-1025.

335 [21]. EN 196-1. European Committee for Standardization. Methods of testing cement. Part
336 1: Determination of strength. Brussels: 2005.

337 [22]. Kollek JJ. The determination of the permeability of concrete to oxygen by
338 Cembereau method, a recommendation. Mater Struct 1989; 22(3):225-230.

339 [23]. Baroghel-bouny V. Caractéristiques des pâtes de ciment et des bétons : Méthodes,
340 Analyse, Interprétations. Paris: LCPC, 1994.

341 [24]. Wee TH, Suryavanshi AK, Tin SS. Evaluation of rapid chloride permeability test
342 (RCPT) result for concrete containing mineral admixture. ACI Mater journal
343 2000;97(2):221-232.

344 [25]. Glasser FP, Marchand J, Samson E. Durability of concrete; Degradation phenomena
345 involving detrimental chemical reactions. Cem Concrete Res 2008;38(2):226-246.

346 [26]. Arya C, Buenfeld NR, Newman JB. Factors influencing chloride binding in concrete.
347 Cem Concrete Res 1990;20(2):291-300.

348 [27]. Han Young M, Hong Sam K, Doo Sun C. Relationship between average pore
349 diameter and chloride diffusivity in various concretes. Constr Build Mater 2006;20(9):725-
350 732.

351 [28]. Cheng A, Huang R, Jiann-Kuo W, Cheng-Hsin C. Influence of GGBS on durability
352 and corrosion behavior of reinforced concrete. Mater Chem and Phy 2005;93(2-3):404-
353 411.

354 [29]. Cho SW, Chiang SC. Measuring, monitoring and modeling Concrete Properties.
355 Netherlands: Springer, 2006.

356 [30]. Iyoda T, Sagawa Y. The effect of curing period on the durability of concrete using
357 blast-furnace slag blended cement. Proceedings of 3rd ACF International Conference.
358 Vietnam, 2008.

359 [31]. Alexander MG, Magee BJ. Durability performance of concrete containing condensed
360 silica fume. Cem Concrete Res 1999;29(6):917-922.

361
362
363
364
365
366

Tables Captions

Table 1: Chemical composition of cement and slag

Table 2: Compressive strength, water absorption by immersion P_W of mortar with and without GBFS

Table 3: Chloride diffusion rate for mortars

Table 4: Pore network characteristicsof mortar with and without GBFS after 360 days of moist curing and after 360 days of diffusion test: threshold pore access radius (r_t) and medium pore radius (r_m)

Table 1: Chemical composition of cement and slag

	SiO_2	CaO	Al_2O_3	MgO	Fe_2O_3	Free CaO	SO_3	Loss of ignition	Na_2O	K_2O	Insoluble residue
OPC	18.4	61.3	5.6	0.9	3.8	0.20	3.3	2.2	0.42	0.78	0.50
GBFS	41.2	42.84	9.19	2.12	3.44	-	0.15	0.2	0.10	0.70	-

Table 2: Compressive strength, water absorption by immersion P_W of mortar with and without GBFS

Mortars	Slag (%)	Compressive strength (MPa) 90 days	Compressive strength (MPa) 360 Days	Water absorption by immersion P_W (%) 90 Days	Water absorption by immersion P_W (%) 360 Days
M0	0	68.6	76.0	15.99	15.72
M30	30	67.2	74.5	17.10	16.76
M50	50	55.7	67.5	18.31	17.90

Table 3: Chloride diffusion rate for mortars

Mortars	Breakthrough time (days)		Effective diffusion coefficient (m^2/s)	
	90 days moist curing	180 days moist curing	90 days moist curing	180 days moist curing
M0	45	52	2.96×10^{-10}	2.78×10^{-10}
M30	73	91	1.19×10^{-10}	0.67×10^{-10}
M50	220	*	0.22×10^{-10}	**

* No appearance of chloride in the cell 2
** Steady state not reached

Table 4: Pore network characteristics of mortar with and without GBFS after 360 days of moist curing and after 360 days of diffusion test: threshold pore access radius (r_t) and medium pore radius (r_m)

	After 360 days moist curing		After 360 days of diffusion test	
	r_t (nm)	r_m (nm)	r_t (nm)	r_m (nm)
M0	31.5	30.5	28	27.3
M30	30.0	28.0	29	27
M50	28.0	25.3	24.5	24.1

Figures Captions

Fig. 1: Experimental setup of diffusion cells.

Fig. 2: Chloride diffusion rate for mortars with GBFS after 90 days (a) and 180 days (b) of moist curing

Fig. 3: Distribution of capillary pore radius for different mortars after 360 days moist curing

Fig. 4: Distribution of capillary pore radius for different mortars after 360 days chloride diffusion

Fig 5: Chloride conduction for mortars with GBFS after 90 and 180 days of moist curing

Fig. 6: Correlation between chloride diffusion coefficient and total charge Q

Fig. 7: Oxygen permeability for mortars with GBFS after 90 and 360 days of moist curing

.

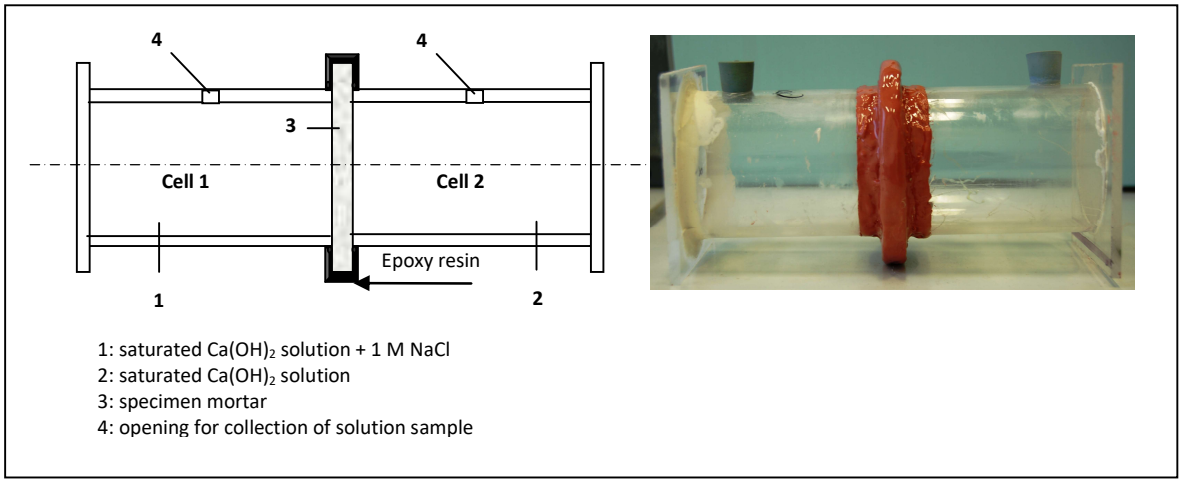

Fig. 1: Experimental setup of diffusion cells.

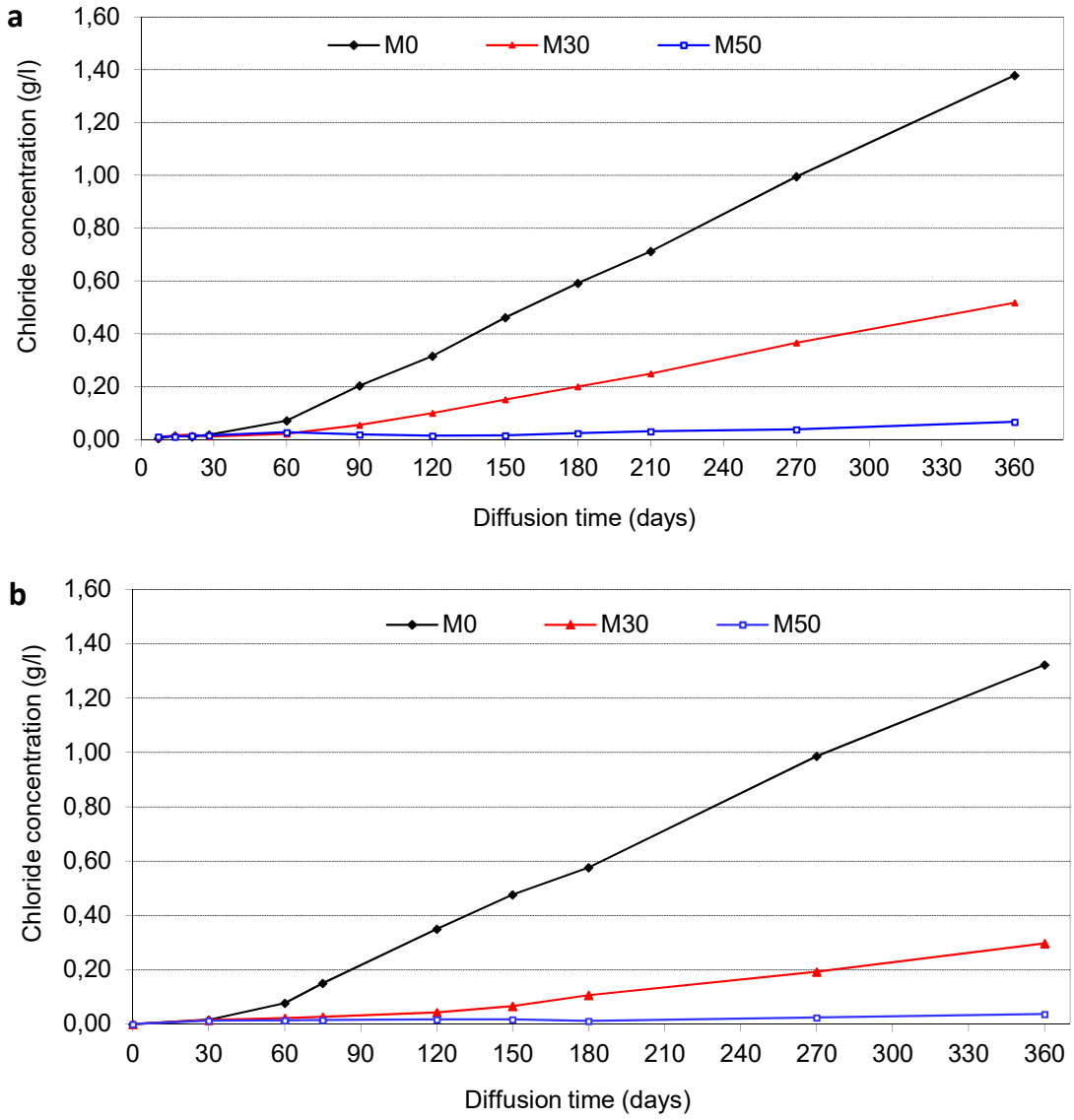

637 Fig. 2: Chloride diffusion rate for mortars with GBFS after 90 days (a) and 180 days (b) of moist
638 curing
639
640
641
642
643
644
645
646
647
648
649
650
651

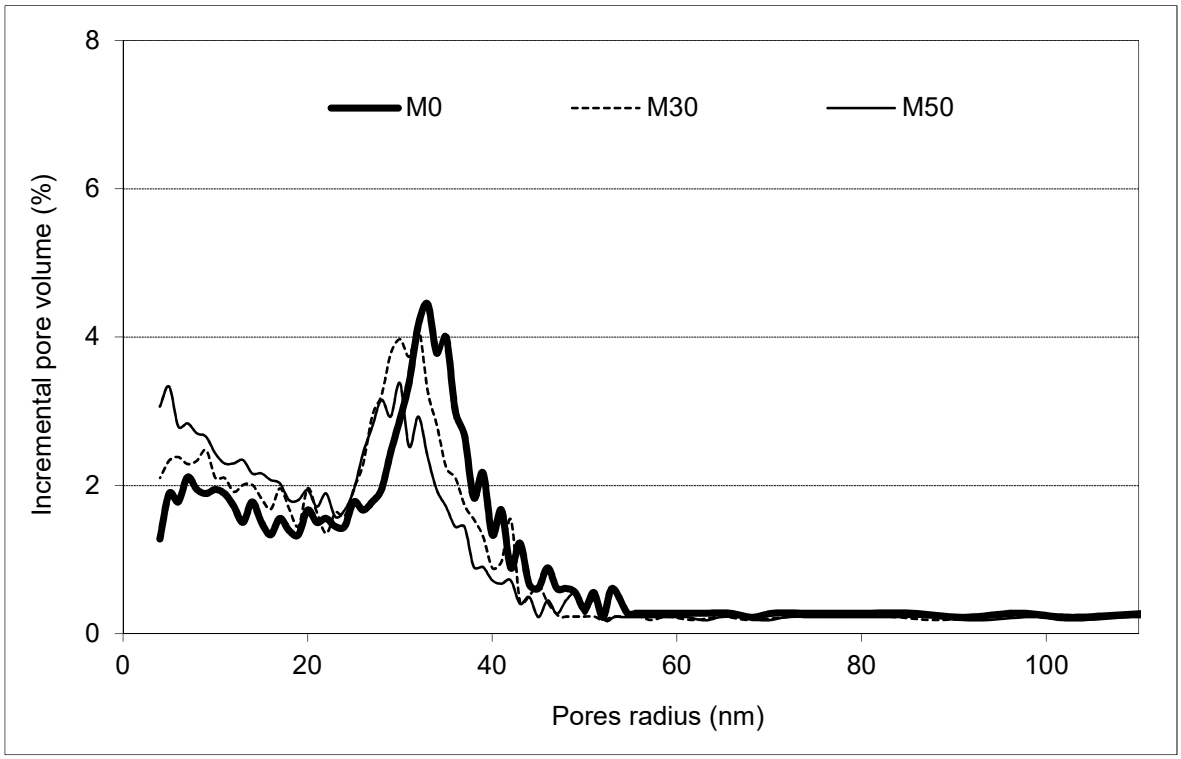

Fig. 3: Distribution of capillary pore radius for different mortars after 360 days moist curing

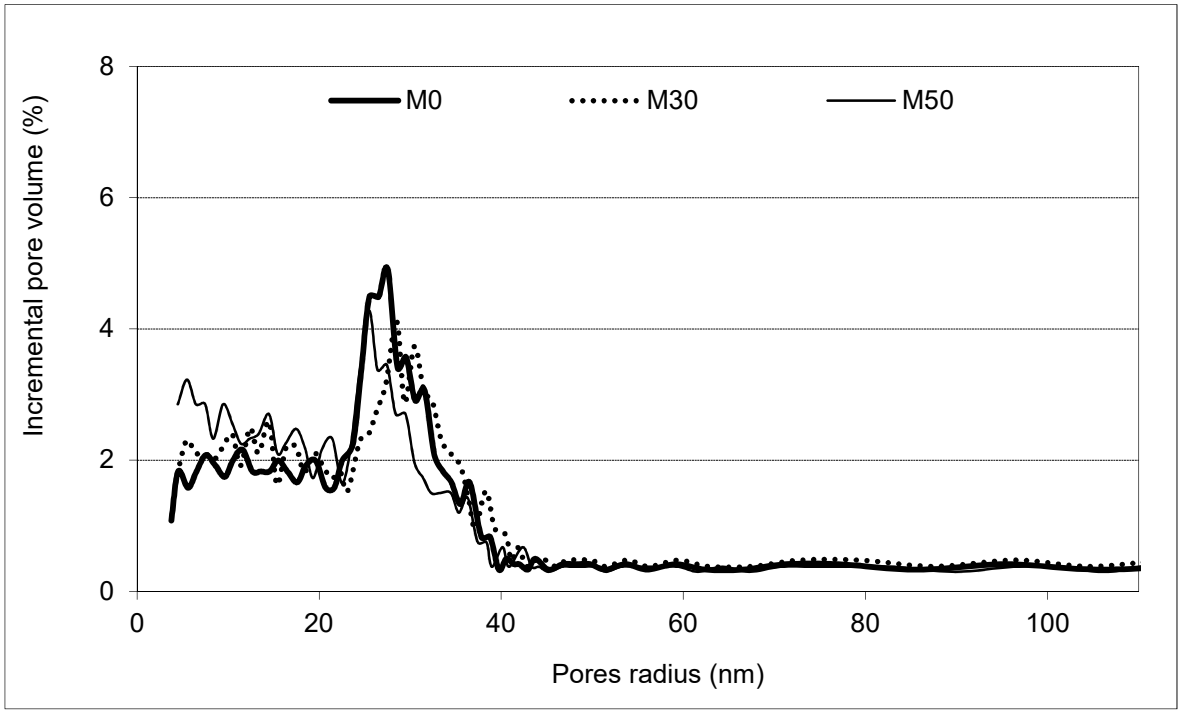

Fig. 4: Distribution of capillary pore radius for different mortars after 360 days chloride diffusion

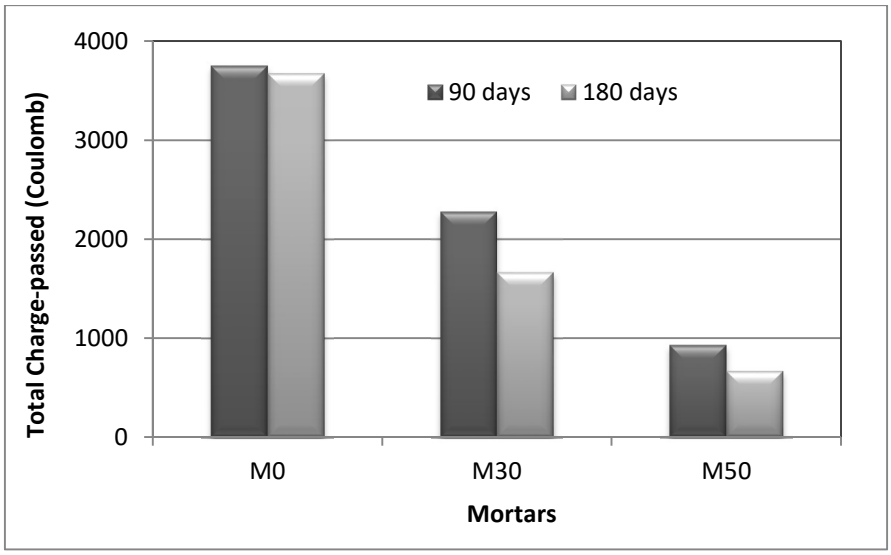

688

689 Fig 5: Chloride conduction for mortars with GBFS after 90 and 180 days of moist curing

690

691

692

693

694

695

696

697

698

699

700

701

702

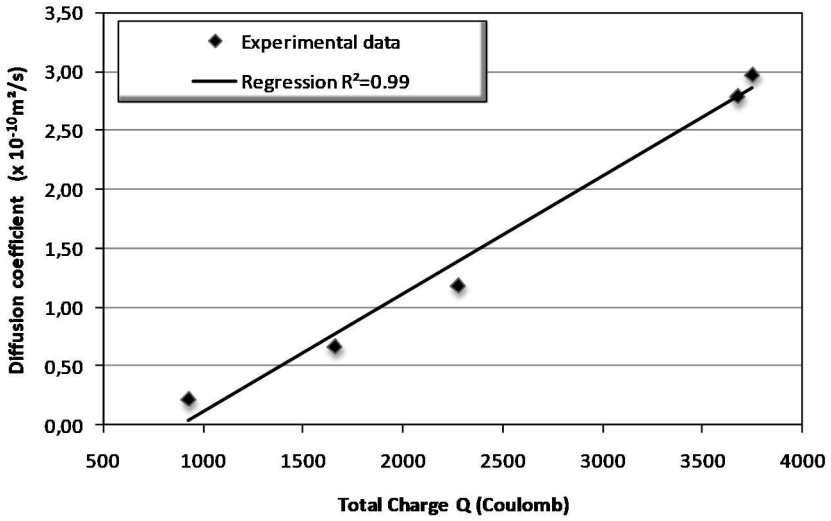

703 Fig. 6: Correlation between chloride diffusion coefficient and total charge *Q*

704

705

706

707

708

709

710

711

712

713

714

715

716

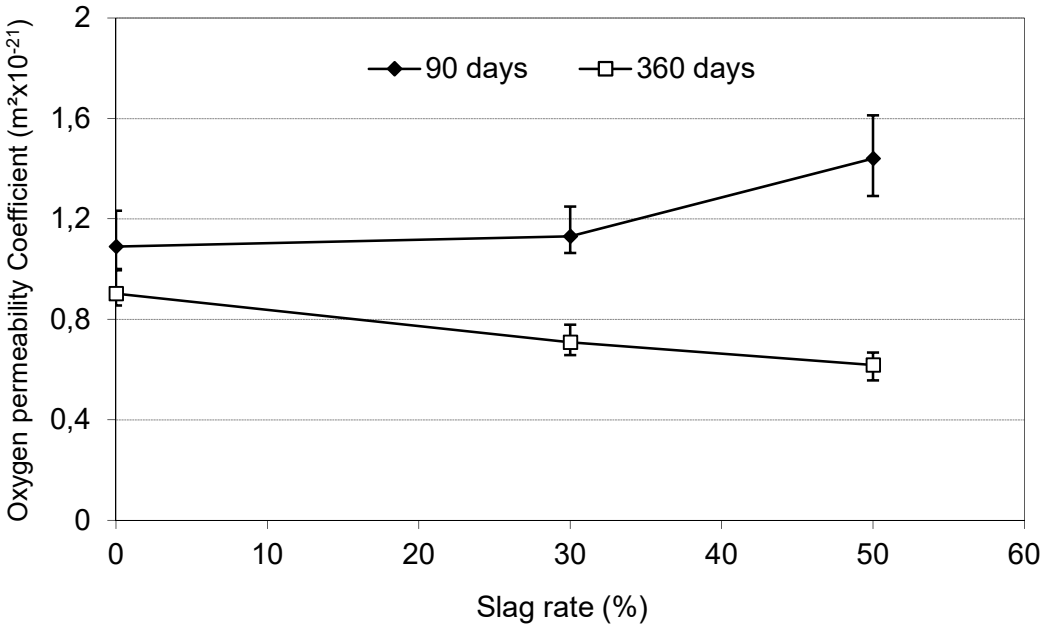

717

718 Fig. 7: Oxygen permeability for mortars with GBFS after 90 and 360 days of moist curing